Kinetics of the CO Oxidation by O_2 and N_2O over $Cu\text{-}Cr/Al_2O_3$

Nico J. J. Dekker, Johan A. A. Hoorn, Sander Stegenga, Freek Kapteijn, Jacob A. Moulijn
Dept. of Chemical Engineering, University of Amsterdam, Amsterdam, The Netherlands

The oxidation of CO by O_2 and N_2O over an oxidized 10 wt. % $Cu\text{-}Cr/Al_2O_3$ catalyst ($Cu:Cr = 1:1$) has been studied by temperature-programmed reactivity measurements (400–550 K) over a wide range of partial reactant pressures, including inhibition by CO_2. The CO oxidation rate is zeroth-order in oxygen and has orders between 0–1 in CO and N_2O, depending on the gas-phase composition. Mechanistic information from literature combined with the kinetic data resulted in the selection of an Eley-Rideal-type of kinetic model without a priori assumptions on rate-determining processes. The model consists of the oxidation of reduced sites by O_2 and/or N_2O, followed by a reaction with CO, yielding a surface intermediate that releases CO_2 in a consecutive step. CO_2 inhibits both by reversible adsorption on oxidized and reduces sites, the latter under formation of the surface reaction intermediate. Apart from the surface oxidation by O_2, the reaction rates of all assumed elementary processes are of the same order of magnitude and, therefore, determine the overall rate. The surface oxidation by oxygen is about four orders of magnitude larger, which explains the zeroth-order in oxygen and the observation that oxygen first reacts with CO before N_2O is able to oxidize CO. The obtained activation energies of the elementary processes agree with values in the literature for corresponding systems.

Introduction

In automotive exhaust gas purification, the monolithic three-way catalyst, based on Pt and Rh, has found a wide application. With still increasing demands, together with decreasing sulfur levels in gasoline fuels, base metal catalysts become attractive as alternative. Recently, we reported the promising three-way behavior of copper-based catalysts (Stegenga et al., 1991).

The idea of using Cr-Cr as active phase is not new, the high activity of Cu-Cr for the CO oxidation was already reported in 1933 by Lory (1933). Later, Shelef et al. (1968), Dwyer (1972), and McCabe and Mitchell (1988) showed that the activity of Cu-Cr for the CO oxidation and NO reduction is comparable with Pt-Rh systems.

Insight in the kinetics of the reaction steps is essential to predict the performance of such catalysts under realistic conditions and to optimize the design of catalytic converters. The best way to develop the kinetic model is achieved by using a sequence of elementary processes, based on available mechanistic information pertaining to the overall process. The fitted derived rate expression is expected to have a validity extending beyond the range of experimental conditions from which it has been selected (Carberry, 1987), especially if the estimated rate parameters have a physical significance (Boudart et al., 1967).

The different reaction mechanisms proposed for Pt-Rh and base-metal catalysts do not allow us to draw parallel kinetic models (Schlatter et al., 1973). In a crude approach, the major difference is the metallic character of the Pt-Rh system in comparison with the oxidized state of the base-metal systems. Therefore, the interaction of the reacting molecules with the active phase will hardly be comparable. The kinetic models are expected to be quite different and have to be determined individually. For instance, the oxidation of CO over Pt is assumed to proceed via a reaction between adsorbed oxygen and an adsorbed CO species in a Langmuir Hinshelwood type of model (Liao et al., 1982), whereas over base-metal catalysts

Correspondence concerning this article should be addressed to F. Kapteijn.
Present address of: J. A. Moulijn, Dept. of Chemical Engineering, Delft University of Technology, Julianalaan 136, 2628 BL Delft, The Netherlands.

it is still unclear whether CO reacts in a similar way in the adsorbed state or from the gas phase in an Eley Rideal type of model (Happel et al., 1977).

In more complex reaction mixtures, like exhaust gases, oxidizing agents, O_2, N_2O, and NO, compete to react with reducing agents, CO and hydrocarbons. The total composition of the reaction mixture will strongly determine the state of the catalyst at the surface. Especially base metals are quite sensitive to reducing or oxidizing conditions and may change considerably in activity (Severino and Laine, 1983; Stegenga et al., 1991). Therefore, this competition of the reactants has to be taken into consideration, since the individual modeling of reactions will not necessarily predict the simultaneous behavior properly.

In view of the above, the steady-state kinetics of the CO oxidation by O_2 and N_2O over a Cu-Cr/Al_2O_3 catalyst has been studied between 400 and 550 K by temperature-programmed reactivity measurements over a range of gas compositions. N_2O, a undesired side product of the NO reduction, was used here to determine its influence on the exhaust gas composition by the reaction with CO. The selected kinetic model is discussed with respect to earlier studies on base-metal catalysts and the physical significance of the rate parameters.

Experimental Method

Catalyst

The catalyst was prepared by pore volume impregnation of γ-Al_2O_3 [Ketjen 000-1.5E (CK 300), $V_p = 0.5$ mL/g, $S_a = 200$ m^2/g, and $d_p = 0.15$–0.25 mm] with an aqueous solution of copper (II) nitrate and chromium (III) nitrate. After drying for 2 h at 393 K, the catalyst was calcined in air up to 773 K (5 K/min, 2 h isothermal), resulting in a 10 wt. % Cu-Cr/Al_2O_3 catalyst with a Cu/Cr ratio 1.

Apparatus

The CO oxidation experiments were performed in an apparatus consisting of a gas-mixing section, a quartz reactor, and a dual-column gas chromatograph to separate mixtures of CO, O_2, N_2O, N_2, NO and CO_2, as described in detail elsewhere (Stegenga, 1991). The reactor (ID = 5.0 mm) was surrounded by an aluminum cylinder, which contained the thermocouple to control the oven temperature.

The CO oxidation is a very exothermal reaction. To improve the heat transfer from the particles to the surroundings, the catalyst bed was diluted with SiC (volume ratio catalyst:SiC = 1:1.1, $d_p = 0.2$–0.5 mm). Additionally, a heat conductive graphite paste was used to improve the thermal contact between the reactor and the aluminum cylinder. Even under the most extreme reaction conditions applied, these measures resulted in a maximum temperature difference between the catalyst bed and the cylinder of less than 1 K. During the kinetic measurements, the thermocouple in the catalyst bed was removed to avoid any disturbance of the flow pattern and to exclude any possible catalytic activity.

Experimental conditions

In all experiments, the total gas flow amounted to 98 μmol/s. By using 100 mg of catalyst, the volume hourly space velocity was 62.000 h^{-1}. The applied absolute pressure was maintained at 1.5 bar by a back-pressure controller.

Three types of experiments have been performed: CO oxidation with O_2, N_2O, and a mixture of O_2 and N_2O. The inhibition by CO_2 was investigated by adding the reaction product. The gas compositions are summarized in Table 1.

For each type of experiment, a fresh catalyst sample was used. Prior to the measurements with O_2 as oxidizing agent (Table 1a), the catalyst was reduced and oxidized in temperature cycles up to 575 K in 1.5% CO–0.5% O_2 and 1% CO–1% O_2, respectively. Prior to the measurements with N_2O as oxidizing agent (Table 1b), the catalyst was pretreated with 0.31% CO and 0.33% NO up to 625 K to bring the catalyst in a state comparable to such as present during the kinetic NO reduction experiments (Stegenga, 1991). Before the combined reactivity measurements (Table 1c), the catalyst was pretreated in an oxidizing environment with 1% CO and 0.8% O_2 up to 600 K.

Various partial pressures of the gases were obtained by adjusting the molar gas flow rates, maintaining a constant total flow rate. The consequence is that the space time W/F_o of a reacting species is varied inversely proportional to its partial pressure.

In the experiments, the temperature was increased linearly (0.5 or 1 K/min) until a conversion around 90% of the limiting component was attained, after which the temperature was decreased by using the same temperature gradient. This procedure avoided exposure of the catalyst to a gas-mixture without oxidizing or reducing agent and resulted in reproducible activity measurements. During the temperature ramp, the product stream was analyzed every 6 minutes.

The CO conversion was calculated by Eq. 1, where only ratios of CO and CO_2 are used:

$$X_{CO} = \frac{CO_{2\,out}/CO_{out} - CO_{2\,in}/CO_{in}}{1 + CO_{2\,out}/CO_{out}} \tag{1}$$

This diminishes the error whenever the absolute sensitivity of

Table 1. Composition of the Reactor Feed Mixtures

1a: Mixtures of CO, O_2 and CO_2

		CO(%)		
		1	2	3
O_2(%)	1	0, 5%	0, 5, 10%	0, 5%
	2	0, 2%	0, 2%	0, 2%
	3	0, 2, 5%	0, 2, 5%	0, 2, 5%

1b: Mixtures of CO, N_2O and CO_2

		CO(%)		
		0.3	0.5	1
N_2O(%)	0.1	0, 2%	0%	0, 2%
	0.3	0, 2%	0%	0%
	0.43	0, 2, 5%	0%	0%

1c: Mixtures of CO, O_2, N_2O and CO_2

CO(%)	O_2(%)	N_2O(%)	CO_2(%)
1	0.35	-	-
1	0.35	0.4	-
1	0.35	0.4	5
0.3	-	0.4	-

the TCD detector slightly changes during the experiment. The derivation of the equation is given in the Appendix A. If no CO_2 is added to the feed, the formula reduces to the more common equation:

$$X_{CO} = CO_{2\,out}/(CO_{out} + CO_{2\,out}) \tag{2}$$

The N_2O conversion was calculated by:

$$X_{N_2O} = N_{2\,out}/(N_{2\,out} + N_2O_{out}) \tag{3}$$

Temperature gradients and diffusion limitations

To obtain intrinsic reaction rate data, which can be interpreted in a simple way, the following requirements have to be fulfilled:

- The precautions, taken to avoid a temperature rise of the catalyst bed, were sufficient to assure isothermal behavior. Hence, the less severe criteria for the absence of intraparticle heat-transfer limitations are automatically satisfied (Carberry, 1987).
- By using the Wheeler-Weisz criterion (Carberry, 1987) and varying the particle size of the catalyst, it was confirmed that intraparticle diffusion limitations were absent.
- The reactor to particle diameter ratio of 20–30 was sufficient to assume a flat velocity profile across the reactor diameter (Chu and Ng, 1989).
- The catalyst bed length to particle diameter ratio of 50–80 allows us to neglect the axial dispersion in the catalyst bed.

The latter two conditions imply that the reactor system can be considered as an ideal plug flow reactor (Gierman, 1988).

Data processing

After the calculation of the CO and N_2O conversions in the experiments, these data sets were fitted on the rate equations by nonlinear regression. The objective function that was minimized was the sum of squares of the residual CO and N_2O conversion, that is, the difference between the observed and calculated value:

$$\text{O.F.} = \sum_i (X_{CO} - \hat{X}_{CO})^2 + \sum_i (X_{N_2O} - \hat{X}_{N_2O})^2 \tag{4}$$

This minimization was achieved by optimizing the rate parameters, expressed in an Arrhenius-type temperature dependency, according to the Simplex and Levenberg-Marquardt methods. To improve the convergence of the minimization routines, a reparametrization of the rate constants was applied according to Eq. 5 (Froment and Hosten, 1981):

$$k,K = \exp\left[A - B\left(\frac{1}{T} - \frac{1}{T_{avg}}\right)\right] \tag{5}$$

where

for k: $A = \ln(k_o N_t) - E_a/(R \cdot T_{avg})$
$B = E_a/R$
for K: $A = \ln K_o - \Delta H/(R \cdot T_{avg})$
$B = \Delta H/R$

The values of the $\ln(k_o N_t)$, E_a, $\ln(K_o)$ and ΔH of the elementary processes were calculated from the estimated parameters A and B.

Since the rate expressions do not yield the conversions in an explicit form, they were calculated by the integration of the coupled differential equations for $\hat{X}_{CO}$ and $\hat{X}_{N_2O}$, derived from the continuity equation (Eq. 6) of a plug flow reactor.

The numerical integration was done by the efficient Bulirsch-Stoer method (Press et al., 1989).

$$\frac{d\hat{X}_A}{dW} = \frac{r(\hat{X}_A)}{F_{Ao}} \quad (A = CO,\ N_2O) \tag{6}$$

Results

$CO + O_2$

In Figure 1A, the CO conversion at 1% O_2 is given as a function of the temperature for three different CO concentrations. Apparently, the CO conversion decreases with increasing concentration. Because the flow of CO was increased to achieve proportionally higher concentrations, the overall

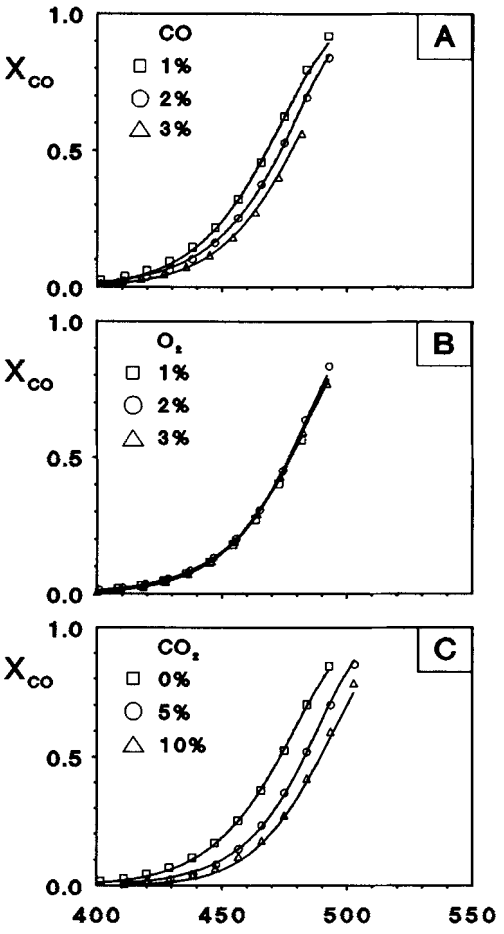

Figure 1. CO conversion as a function of the temperature.

A. As a function of the CO concentration (1% O_2).
B. As a function of the O_2 concentration (3% CO).
C. As a function of the CO_2 concentration (2% CO and 1% O_2).

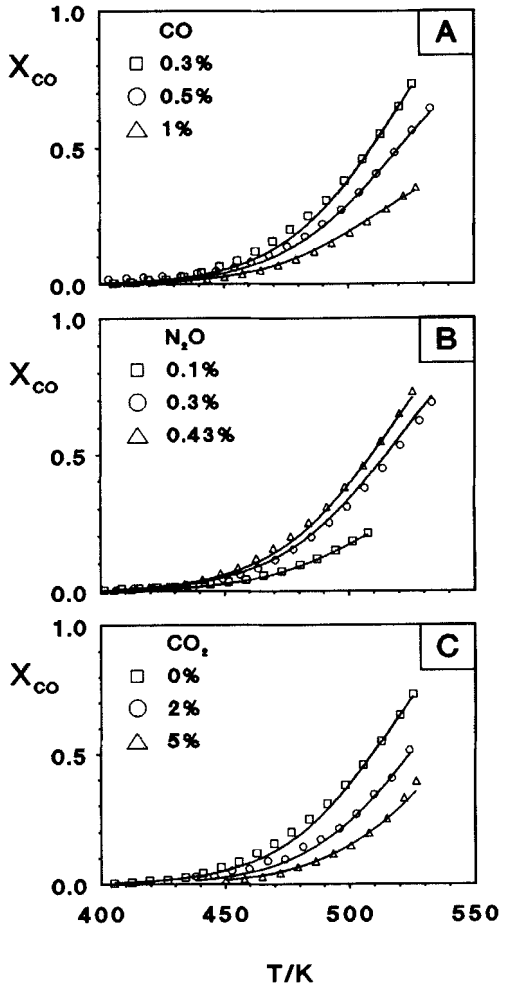

Figure 2. CO conversion as a function of the temperature.

A. As a function of the CO concentration (0.43% N_2O).

B. As a function of the N_2O concentration (0.3% CO).

C. As a function of the CO_2 concentration (0.3% CO, 0.43% N_2O).

amount of CO converted in these experiments does increase with the CO partial pressure, but not linearly. Other oxygen pressures gave similar results.

Figure 1B contains results of the effect of the oxygen pressure on the CO conversion at constant CO pressure as a function of the temperature. The reaction rate is independent of the oxygen pressure over the whole range of conditions studied, even at high oxygen conversion levels.

The addition of CO_2 clearly inhibits the reaction rate at all experimental conditions (Figure 1C).

$CO + N_2O$

In Figure 2A, the CO conversion at constant N_2O is plotted for various CO concentrations. It is clearly seen that the decrease in CO conversion at increasing CO concentrations is larger than the CO oxidation by O_2 (Figure 1A).

Figure 3 shows that at low N_2O concentration, the N_2O conversion is nearly independent of the CO concentration. On the other hand, at high N_2O concentrations, the CO conversion becomes more or less independent of the N_2O concentration (Figure 2B). These figures show that the orders in CO and N_2O depend on the CO/N_2O ratio: at high CO/N_2O ratios the N_2O reaction rate is independent of the CO concentration, while at low CO/N_2O ratios the CO reaction rate becomes almost independent of the N_2O concentration. At intermediate CO/N_2O ratios, the reaction rate of CO and N_2O increase with N_2O and CO partial pressures, respectively.

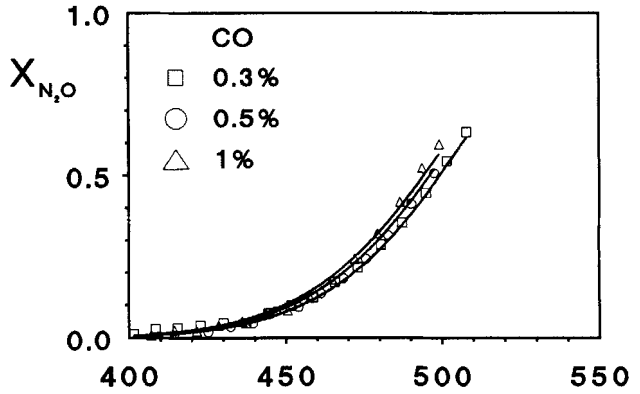

Figure 3. N_2O conversion as a function of the temperature and CO concentration (0.1% N_2O).

In these experiments, inhibition by CO_2 was found (Figure 2C). Compared to the CO oxidation by O_2, the inhibition is stronger and exhibits another temperature dependency.

$CO + O_2 + N_2O$

Several CO oxidation experiments have been performed in the presence of a mixture of O_2 and N_2O. In Figure 4A, the O_2 and N_2O conversion are given for a reaction mixture of 0.35% O_2 and 0.4% N_2O at 1% CO as a function of the temperature. It is clear that the N_2O reduction increases considerably around 90% O_2 conversion levels. Apparently, CO reacts preferably with O_2, after which the remaining CO reacts with N_2O.

The individual oxidation rates of N_2O and O_2 were determined by performing experiments with comparable $CO + O_2$ and $CO + N_2O$ mixtures (Figure 4B). From the comparison with Figure 4A, it is clear that the CO oxidation by O_2 is not influenced by the presence of N_2O, while the N_2O reduction is strongly inhibited by O_2.

The product inhibition was quantified by adding 5% CO_2 to the feed (Figure 4A). The reduction of both O_2 and N_2O were inhibited, as expected from the experiments with the binary $CO + O_2$ and $CO + N_2O$ mixtures. In this case too, the N_2O reduction starts appreciably around 90% O_2 conversion levels.

Kinetic Model

Apparent reaction order

Different kinetic results have been reported in the literature for the CO oxidation with O_2 over copper-based catalysts. In agreement with the results of this study, in general a zeroth reaction order in oxygen and a positive order, less than one,

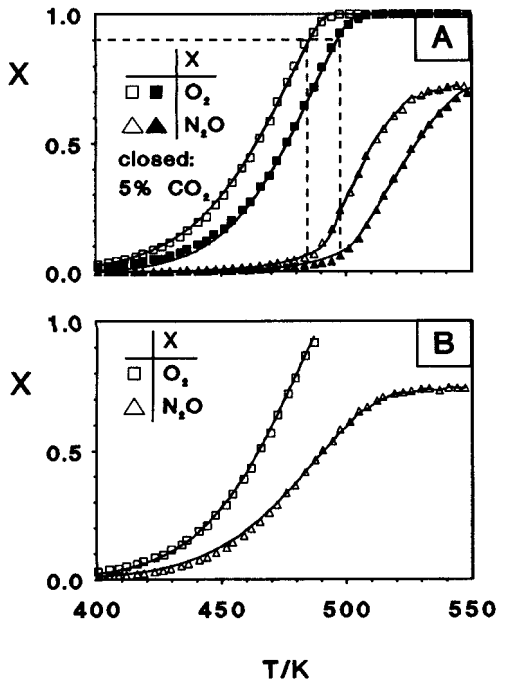

Figure 4. O_2 and N_2O conversion as a function of the temperature.

A. 1% CO, 0.35% O_2, 0.4% N_2O, closed symbols with 5% CO_2.

B. □ : O_2 conversion in 1% CO-0.35% O_2, △ : N_2O conversion in 0.3% CO-0.4% N_2O.

in CO was found. The apparent activation energies range from 50–126 kJ/mol (see Table 2). Only Cu-zeolites showed deviating results: the reaction rates over these catalysts were first-order in oxygen and zeroth-order in CO (Miro et al., 1987). After treatment under extreme conditions (see footnote, Table 2), these catalysts exhibited the more commonly found reaction orders. The effect of CO_2 on the kinetics has hardly or not been studied. Some investigations reported no effect, others a slight inhibition by CO_2.

For the oxidation of CO by N_2O over oxidized Cu catalysts, no comparable publication was found. Over Cr_2O_3, the reaction rate of N_2O was zeroth-order in CO, 0.8 in N_2O, and -0.2 in CO_2 at 545 K (Krupay and Ross, 1978), which is in the same order of magnitude as found in this investigation at high CO/N_2O ratios.

Reaction mechanism and active phase

The CO oxidation over copper-based catalysts is considered to proceed according to an oxidation-reduction mechanism of the active phase (Shelef et al., 1968; Hertl and Farrauto, 1973; Miro et al., 1984, 1987; Halasz et al., 1990).

The activity of the Cu-Cr/Al_2O_3 catalyst for the CO oxidation by O_2 is attributed to Cu, the activity of Cr is much lower (Yu Yao, 1975; Severino and Laine, 1983; Laine et al., 1990), as confirmed by measurements at our laboratory (Stegenga et al., 1991; Stegenga, 1991). Chromium is thought to stabilize the Cu phase against sintering (Yu Yao, 1975; Laine et al., 1990; Madhusadhan and Shankar, 1988) and to limit the extent of reduction by formation of a $CuCr_2O_4$ phase (Tonner et al., 1984; Severino et al., 1986).

Possible redox couples under working conditions are $Cu^+ - Cu^{2+}$, $Cu^0 - Cu^{2+}$, and $Cu^0 - Cu^+$. After oxidation by O_2 copper is mainly present as Cu^{2+} (Yu Yao, 1975, Severino et al., 1986; Miro, 1987; Laine and Severino, 1990). The oxidation state under working conditions is only slightly lowered, which makes the redox couple $Cu^+ - Cu^{2+}$ for the CO oxidation by O_2 the most probable (Deen et al., 1976; Laine and Severino, 1990; Bijsterbosch et al., 1991).

N_2O is often used for the determination of Cu^0 surface areas. At temperatures between 290 and 370 K Cu^0 at the surface is oxidized to Cu^+, while at higher temperatures bulk oxidation occurs and Cu^{2+} is formed (Evans et al., 1983; Luys et al., 1989).

The CO oxidation by N_2O of our catalyst was strongly activated by a reduction with an excess CO at 470 K (0.3% CO and 0.1% N_2O, 100% N_2O conversion). After this reduction, 40% N_2O conversion was reached at 330 K, while during the kinetic measurements the temperature had to be raised up to 485 K to reach this level. This high activity sustained during heating and cooling under these reducing conditions can be ascribed to the $Cu^0 - Cu^+$ redox couple. Because during our kinetic experiments, excessive reduction was avoided, the catalyst was kept in an oxidized state, and the existence of Cu^0 in a redox couple can be excluded. Therefore, it is assumed that also in the case of N_2O as an oxidizing agent, the redox couple $Cu^+ - Cu^{2+}$ is operative.

The oxidation by O_2 probably occurs via dissociative ad-

Table 2. Overview of Kinetic Investigations, $r_{CO} = k\,[CO]^a\,[O_2]^b\,[CO_2]^c$

Catalyst	T(K)	a	b	c	Ea(kJ/mol)	Reference
CuO	345–410	0.3–0.8	0	<0	73–106	Thomas et al. (1969)
CuO	425–475	0.7	0	0	92	Yu Yao (1975)
$CuCr_2O_4$	425–475	0.7	0	0	97	Yu Yao (1975)
$BaCuO_2$	425–445	1.2	0	-	63	Halasz et al. (1990)
Cu-Cr/Al_2O_3	475–675	0.7	0	-	-	Schlatter et al. (1973)
CuO.$CuCr_2O_4$	420	1	0	−0.33	84	Hertl and Farrauto (1973)
Cu-Y Zeolite	625–725	0	1	-	63	Pentunchi and Hall (1983)
Cu-Y Zeolite*	425–625	1	0	-	56	Miro et al. (1984)
Cu-Mordenite	475–525	0	1	-	92	Miro et al. (1987)
Cu-Mordenite	525–595	1	0	-	126	Miro et al. (1987)
Cu-Mordenite*	475–595	1	0	-	50	Miro et al. (1987)
Cu/Al_2O_3	423	0.5	0.2	-	70	Choi and Vannice

*Zeolite after reduction by CO (1,025 K) and oxidation by O_2 (775 K).

Table 3. Elementary Processes Considered

	Oxidation of the Catalyst							
k_1	O_2	+	2 ■	→	2 O-■			
k_2	N_2O	+	■	→	O-■	+	N_2	
	Reduction of the Catalyst by CO from Gas Phase							
k_3	CO	+	O-■	→	CO_2-■			
	Reversible CO Adsorption on Reduced Sites							
K_4	CO	+	■	⇌	CO-■			
	Reduction of the Catalyst by Surface Reaction							
k_5	CO-■	+	O-■	→	CO_2-■	+	■	
	Reversible CO_2 Adsorption							
K_6	CO_2	+	■	⇌	CO_2-■			
K_7	CO_2	+	O-■	⇌	CO_3-■			

sorption (Gruzalski et al., 1983; Hupkens et al., 1986; Habraken et al., 1980). Isotopic experiments showed that the rate of exchange of $Cu^{16}O$ at 625 K by $^{18}O_2$ under the formation of $^{16}O^{18}O$ and $^{16}O_2$ is low (Duprez et al., 1990) and can be neglected compared to the reduction rate by CO. Therefore, the oxidation of the catalyst is represented as an irreversible process, which also holds for the oxidation by N_2O (Spitzer and Lüth, 1984; Habraken et al., 1980). Both O_2 and N_2O are believed to oxidize the same sites (Habraken and Bootsma, 1979; Spitzer and Lüth, 1984). In this article, the oxidized form of the site is represented by O-■ and the reduced form by ■.

The oxidized catalyst can be reduced by CO either from the gas phase [Eley Rideal model (Happel et al., 1977)] or by adsorbed CO[Langmuir Hinshelwood model (Habraken et al., 1980)] under the formation of CO_2-■.

The CO oxidation over Pt/Al_2O_3 catalysts proceeds by a Langmuir Hinshelwood model (Liao et al., 1982). Typically, at low CO concentrations the reaction rate increases with the CO concentration, while at high concentrations it passes through a maximum due to the strong CO adsorption at the Pt surface. For a Cu/Al_2O_3 catalyst at equal conditions, the reaction rate still increases even up to 5% CO (Liao et al., 1982), indicating a weak adsorption of CO (Balkenende, 1990) or reaction of CO from the gas phase. By *in-situ* FTIR, CO adsorption has been observed on Cu^+ sites under reducing conditions. In the presence of O_2, this CO adsorption was absent although CO reacted to CO_2. This strongly suggests that CO does not have to adsorb before reacting (Bijsterbosch et al., 1991). The Eley Rideal model has been proposed for various base-metal catalysts like CuMn oxide (Happel et al., 1977), NiO (Conner and Bennett, 1976), MgO (Kobayashi et al., 1987), ZnO (Kobayashi et al., 1988), Cr_2O_3 (Shelef et al., 1968), and Cu/Al_2O_3 (Eckert et al., 1973), and was chosen as the basis for our model.

CO_2 can adsorb in several manners at different sites at base-metal oxides under formation of carbonates and mono- and bidenates (Hertl and Farrauto, 1973; Busca, 1987; Davydov, 1990), retarding the CO oxidation by blocking active sites. Similar structures were found as the reaction product of the CO oxidation (Busca, 1987; Bijsterbosch et al., 1991). Exposure of the catalyst to CO_2 yields a labile-adsorbed CO_2 species, which desorbs under evacuation at 300 K (Busca, 1987), and a more strongly held CO_2 (Jackson, 1989). Isotopic exchange experiments (Jackson, 1989) indicated that the adsorption of CO_2 on O-■ yields the labile species, indicated here as CO_3-■. The reactions of CO with O-■ or CO_2 with ■ yield the same surface species, denoted as CO_2-■ (Busca, 1987; Bijsterbosch et al., 1991). CO_2 is not able to oxidize Cu^+ (Miro et al., 1987; Tonner et al., 1984; Kinnaird et al., 1988), which means that the reduction of the catalyst by CO must be an irreversible process (Hertl and Farrauto, 1973; Happel et al., 1977).

Based on the experimental evidence presented in the literature, the possible elementary processes that should be considered in kinetic modeling are summarized in Table 3. Steps 1 and 2 represent the irreversible oxidation of the reduced sites by O_2 and N_2O. Step 3 is the reaction of CO from the gas phase with an oxidized site, whereas via steps 4 and 5 CO has to adsorb first before reacting with oxygen on an adjacent site. Steps 6 and 7 account for the reversible adsorption of CO_2 on reduced and oxidized sites, respectively. With these elementary processes, various kinetic models can be proposed and rate expressions be derived (Froment and Bischoff, 1990). In view of our FTIR results (Bijsterbosch et al., 1991), we selected a model without steps 4 and 5. In Appendix B, the derivation of the reaction rate equations of this model is given.

Parameter Estimation

CO + O₂

The CO oxidation is zeroth-order in O_2, even at very low O_2 concentrations (Figure 1B), which indicates that the oxidation process is a very fast reaction. The rate-determining process will be the reaction between CO and O-■, followed by the decomposition of CO_2-■. The decomposition of CO_2-■ must influence the overall rate; otherwise, a reaction order

Table 4. Parameter Values Determined for the Elementary Processes

	Data of Table 1a				
	Number of data points: 276 Mean SSR: 2.3e-4 Standard deviation conversion: 1.5e-2				
	ln (K_o)	ΔH kJ/mol	ln (k_oN_t)	E_a kJ/mol	value* mol/kPa·s·g
k_3N_t			10.0	86	4.2e-6
$k_{-6}N_t$			12.6	91	1.5e-5**
K_7	−14.4	−49			

	Data of Table 1b (N_t* 0.30) and 1c				
	Number of data points: 746 Mean SSR: 1.3e-4 Standard deviation conversion: 1.1e-2				
	ln (K_o)	ΔH kJ/mol	ln (k_oN_t)	E_a kJ/mol	Value* mol/kPa·s·g
$k_1s\ N_t$			4.84	30†	4.6e-2
k_2N_t			8.84	82	3.7e-6
k_3N_t			6.21	72	3.7e-6
k_6N_t			12.7‡	95‡	5.6e-6‡
$k_{-6}N_t$			11.9	90	9.7e-6**
K_6	0.74	5			
K_7	−14.4	−49			

*At 460 K. †Fixed value, see text.
**Dimension mol/s·g. ‡Calculated from k_{-6} and K_6.

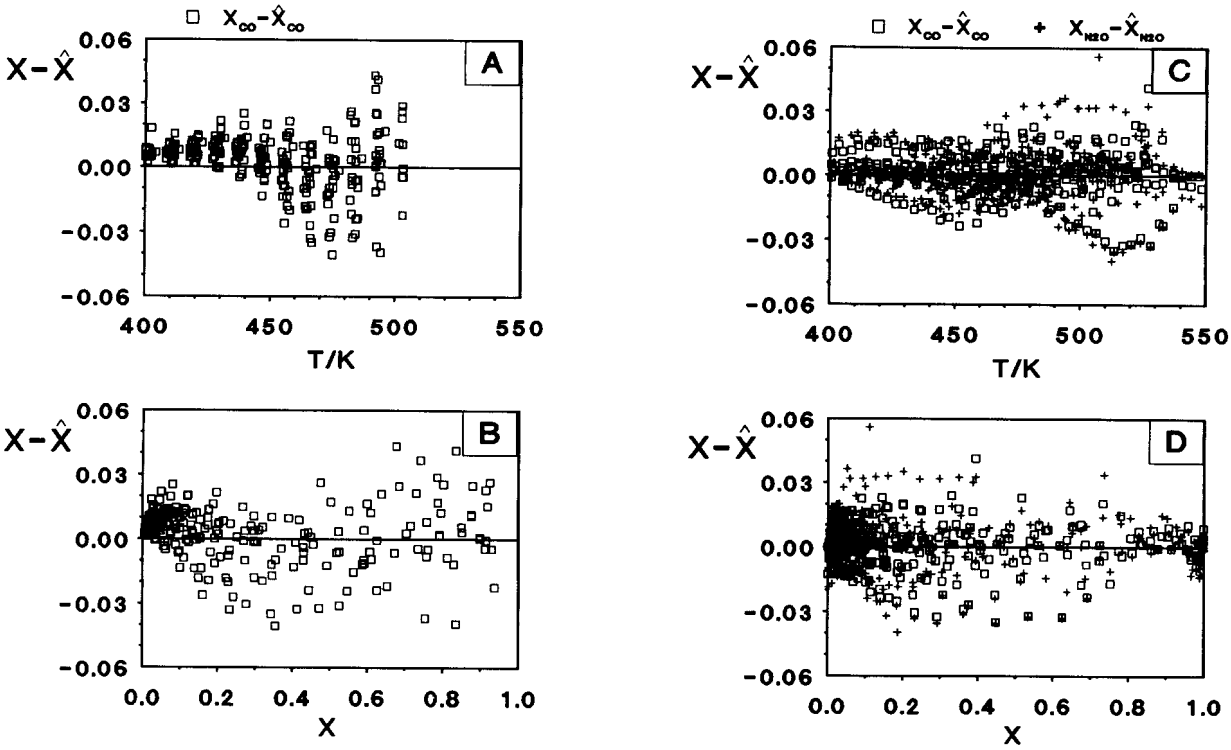

Figure 5. Residual (observed-calculated) conversion as a function of the temperature and conversion.

A and B. CO oxidation by O_2 (Table 1a).
C and D. CO oxidation by O_2 and/or N_2O (Tables 1b-1c).
A and C. Residuals as a function of the temperature.
B and D. Residuals as a function of the conversion.

closer to one in CO is expected. Due to the very fast oxidation by O_2, the number of reduced sites will be very low. Therefore, the adsorption of CO_2 from the gas phase in the presence of O_2 will occur mainly on oxidized sites under formation of CO_3-■. The number of oxidized sites hardly depends on the O_2 concentration, which explains that the CO_2 inhibition appeared to be independent of the O_2 concentration.

From this set of experimental data, only the parameter values of k_3, k_{-6} and K_7 could be determined. Since the reaction was zeroth-order in O_2, the rate constant k_1 of the oxidation by O_2 could not be estimated by these experiments. In Table 4, the calculated values of the reaction rate constants of the elementary processes are given. The drawn curves in the Figures 1A-1C are based on these values. For a better impression how well the model fits, plots of the residual CO conversion as a function of the temperature and of the CO conversion are given in Figures 5A and 5B. The mean SSR value indicates an average standard deviation of 0.015 between the calculated and the observed CO conversion.

$CO+N_2O$

The reaction rate of CO with N_2O is lower than that with O_2 (Figure 4B). This must be attributed to the lower rate of oxidation of Cu by N_2O compared to O_2 (Giamello et al., 1984). From the observed reaction orders in CO and N_2O, it is clear that both the oxidation and reduction of the catalyst determine the rate of the overall process. If the CO/N_2O ratio is varied from low to high, the rate-determining process changes from the reduction to the oxidation process of the catalyst, respectively. Compared to the CO oxidation by O_2, the CO_2 inhibition of the CO oxidation by N_2O is stronger and exhibits a different temperature dependency. This means that, besides adsorption on O-■, CO_2 must adsorb also on a reduced site, ■.

The parameter values of k_2, k_3, k_{-6} and K_6 were determined by the data of these experiments.

$CO+O_2+N_2O$

For the determination of the relative reaction rate constants for the oxidation of the catalyst by O_2 compared to N_2O, a mixture of these gases was used for the oxidation of CO (Table 1c, Figure 4A). Compared to the experiments with only one oxidizing agent under similar conditions, it appears that the oxidation of O_2 is hardly influenced by the presence of N_2O, while the N_2O reduction is strongly inhibited by O_2 (compare Figure 4A with 4B). Apparently, O_2 and N_2O competitively oxidize the same type of site, while the rate constant for the oxidation by O_2 (k_1) is much higher than for N_2O (k_2). Only above 90% O_2 conversion levels, the concentration of O_2 becomes sufficiently low at the end of the catalyst bed for N_2O to compete in the oxidation of reduced sites. At higher temperatures this bed section rapidly increases, which is indicated by the steep increase in the N_2O conversion (Figure 4A). Due to this region of competition between the oxidizing agents, an estimation of the parameter value k_1 could be obtained.

For the parameter estimation, the data of Tables 1b and 1c

were combined. Due to the different pretreatment procedures, the activity of the series 1b amounted to about 30% of that of the series 1c. Therefore, the relative catalyst activity between the series 1b and 1c was allowed to vary in the minimization. Since the CO_2 inhibition by adsorption on oxidized sites was determined by the $CO + O_2$ experiments, the parameters of K_7 were fixed at these values. The estimated parameter values of k_1, k_2, k_3, k_{-6} and K_6 are given in Table 4. The SSR value was not affected strongly by varying E_{a1} between 25–55 kJ/mol and was fixed at 30 kJ/mol (Habraken et al., 1980; Balkenende, 1990).

The average standard deviation between the observed and calculated conversion levels amounts to 0.011. The residual plots of the conversion as a function of temperature and conversion level are given in Figures 5C-D. The drawn curves in the Figures 2–4 indicate the good correspondence between the model and the experimental data.

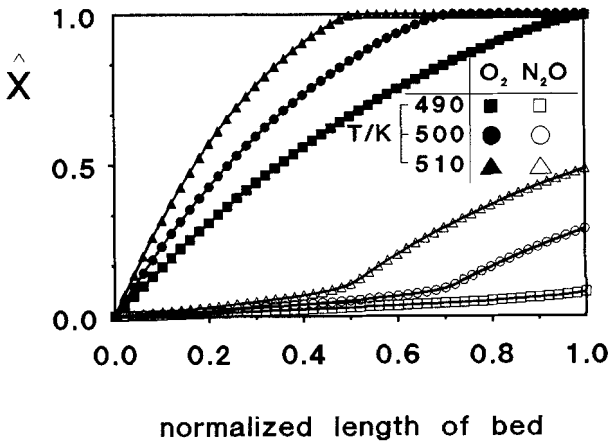

Figure 6. Calculated O_2 and N_2O conversions as a function of the normalized bed length at three temperatures (1% CO, 0.35% O_2, and 0.4% N_2O).

Discussion

The proposed model describes the activity of the catalyst very well as a function of the temperature and the CO, O_2, N_2O and CO_2 partial pressures. This is confirmed by the random distribution of the residuals around zero as a function of the temperature and conversion (Figure 5); this is also the case as a function of the partial pressures (not shown).

To verify whether CO adsorption on reduced sites plays a kinetically significant role, step 4 was added to the selected kinetic model. After regression, the value of K_4 turned out to be negligible within the experimental error. Besides, the SSR had not decreased by incorporation of this additional process, which indicates that the adsorption of CO must be very small. This can directly be seen from Figure 3, since even at low N_2O concentrations (the highest number of reduced sites), no decrease in the N_2O reaction rate was found at increasing CO concentration. So, the adsorption of CO does not affect the reaction rate significantly and was excluded as a relevant elementary process.

In Table 4 the estimated values for the parameters of the elementary processes are given. At first, the parameters were estimated by fitting the data of Tables 1a-c separately. From the comparison of these three parameter sets, it followed that most parameters for equal elementary processes were in the same range of magnitude, except for two parameters.

The value of E_{a3} for the CO oxidation by O_2 of Table 1a was higher compared with the other E_{a3} values. This was attributed to the reduction-oxidation pretreatment, which activated the catalyst. Both the values of the $\ln(k_{o3}N_t)$ and E_{a3} increased by this treatment. Because of the correlation between these two parameters, the values of k_3N_t at 460 K were fairly similar (Table 4).

Also, the activity of the catalyst at 0.3% CO and 0.4% N_2O was lowered by the pretreatment with CO-NO. This was attributed to a decrease in the number of active sites. By combining the data of the experiments of Tables 1b and 1c as one data set, it was determined that the number of active sites decreased to 30%. This parameter set describes the CO oxidation by O_2 of Table 1c also very well, which confirms that the differences in E_{a3} and $\ln(k_{o3}N_t)$ must indeed be attributed to the reduction-oxidation pretreatment.

The rate constant values at 460 K in Table 4 are all of the same order of magnitude, except for k_1 which is four orders of magnitude larger. This explains the zeroth-order dependency in oxygen and the influence of both the CO and N_2O partial pressure on the reaction rate. From these values it is also evident that the elementary processes 2, 3 and -6 together will determine the overall rate. So, it is not possible to assume a single rate-determining process in this reaction.

The estimated activation energies for the oxidation steps are in agreement with other studies. The activation energy of the oxidation by O_2 (E_{a1}) was determined to be in the range of 25–55 kJ/mol, which is in the same range of magnitude as found on single crystal Cu surfaces at temperatures above 470 K, where a considerable oxidation had taken place (Habraken et al., 1980; Balkenende, 1990). The activation energy for the oxidation of a reduced site by N_2O (E_{a2}, 82 kJ/mol) is close to the values determined over copper oxide surfaces by Dell et al. (84 kJ/mol, 1953), Winter (100 kJ/mol, 1970), and Schiavello et al. (96 kJ/mol, 1974).

The product inhibition had to be ascribed to adsorption of CO_2 on two different type of sites. The ΔH_7 for the exothermal adsorption of CO_2 on oxidized sites was estimated to be -49 kJ/mol, which is in agreement with the low stability of the formed CO_3-■ (Busca, 1987; Jackson, 1989). Because $\ln(K_{o7})$ equals $\Delta S_7^o/R$, the standard entropy change for the CO_2 adsorption on oxidized sites can be calculated. For this purpose, K_{o7} must be expressed in atm^{-1}, since the thermodynamic reference state is 1 atm. The value of $\Delta S_7^o = -82$ J/mol·K agrees well with the rule and guideline for an adsorption process, given by Boudart et al. (1967), indicating the adequacy of the kinetic modeling:

Rule: $0 < -\Delta S_7^o < S^o(CO_2)$

Guideline: $41.8 < -\Delta S_7^o < 51.1 - 1.4(\Delta H_7^o)$

The estimated value of ΔH_6 was around zero, so this process cannot be considered as an adsorption process. Moreover, the high activation energy E_{a6} of 95 kJ/mol is highly unusual for an adsorption process. Therefore, the formation of CO_2-■ must be considered as a reaction of CO_2 with a reduced site. The E_{a-6} for the decomposition of the CO_2-■ complex was determined to be about 90 kJ/mol for both the CO oxidation by O_2 as well as N_2O, supporting the proposed model.

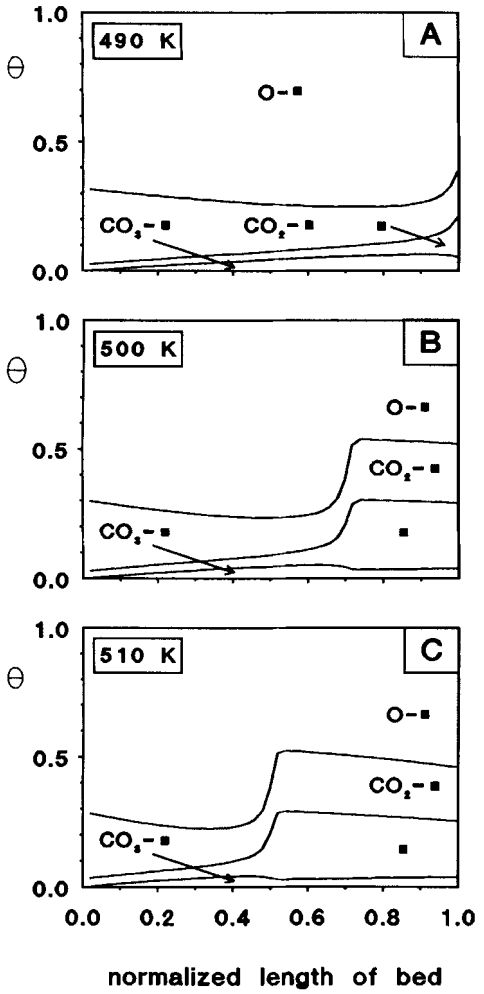

Figure 7. Calculated cumulative fractional surface occupation as a function of the normalized bed length at three temperatures (1% CO, 0.35% O_2, and 0.4% N_2O).

A. 490 K; B: 500 K; G. 510 K.

Using the parameter values of Table 4, the conversion levels along the catalyst bed (Figure 6) and the axial distribution of surface species (Figure 7) were calculated. This was done for the experiment with both O_2 and N_2O as oxidizing agents as a function of the normalized catalyst bed length at three temperatures around the start of the N_2O reduction. These figures give a clear picture of the state of the catalyst during the measurements.

At 490 K 100% O_2 conversion is reached near the end of the catalyst bed, whereas the N_2O conversion only slowly increases along the catalyst bed (Figure 6). At higher temperatures the 100% O_2 conversion is reached much earlier in the catalyst bed, after which a fast increase of the N_2O conversion is calculated.

In Figure 7 the surface occupations are given of ■, O-■, CO_2-■ and CO_3-■. It is clearly seen that at 490 K $\theta_{O\text{-}■}$ remains rather constant up to almost complete O_2 conversion levels and $\theta_■$ stays very low. At higher temperatures $\theta_{O\text{-}■}$ decreases sharply to a lower constant level, whereby $\theta_■$ increases. In this part of the catalyst bed the $\theta_■/\theta_{O\text{-}■}$ is determined by the CO/N_2O ratio. Increasing the temperature leads to a further shift of this front to the beginning of the catalyst bed, by which the section where the N_2O reduction takes place, increases.

Since the CO_2 concentration is rather low, the $\theta_{CO_3\text{-}■}$ does not exceed 5%. The occupation by $\theta_{CO_2\text{-}■}$, formed as reaction product of CO with O-■ and CO_2 with ■, is much higher. Below 100% O_2 conversion the contribution by the reaction of CO_2 with reduced sites is very low and CO_2-■ is formed mainly as the reaction product of the CO oxidation. Near complete O_2 conversion $\theta_■$ strongly increases, which results in an increase in $\theta_{CO_2\text{-}■}$ due to the reaction of CO_2 with reduced sites (Figures 7B–7C).

These simulations, based on the selected model, give a nice insight into the state of the catalyst under the conditions of combined reactions. By consumption of limiting reactants the surface coverage changes considerably over the length of the bed under isothermal conditions. It should be kept in mind that the calculated values of the rate constants apply to an oxidized catalyst system since special care was taken to avoid excessive reduction. This was successful in view of the consistent set of parameters that was obtained. Reduced Cu-Cr catalysts are more active and probably exhibit other kinetic behavior (Pentunchi and Hall, 1983), but former experiments showed that the activity of such reduced catalysts slowly returned to the level of an oxidized sample. Therefore, the kinetic behavior of the oxidized system was chosen as the subject of this study.

Conclusions

The results presented show the applicability of kinetic modeling based on elementary processes, selected on the basis of mechanistic studies, pertaining to the overall process of the CO oxidation by O_2 and N_2O over an oxidized $Cu\text{-}Cr/Al_2O_3$ catalyst. This model predicts excellently the steady-state behavior of the catalyst over a wide range of operating conditions. By the temperature-programmed reactivity approach (up and down), the reproducibility of the rate vs. temperature is automatically checked and hysteresis phenomena could be excluded. The large variation in temperature precluded the *a priori* assumption of a single rate-determining process and permitted us to change the rate-determining process. The latter clearly occurs in mixtures with CO, O_2, and N_2O as a function of the temperature and even as a function of the catalyst bed length. The temperature dependency of the estimated rate parameters (activation energies) corresponds well with values reported in the literature, supporting the selected model. In this model, reduced sites are oxidized by O_2 or, at a lower rate, N_2O. These oxidized sites react with gas-phase CO, under the formation of a surface species that decomposes into CO_2 and a reduced site. The inhibition by CO_2 occurs by reversible adsorption on oxidized sites or by reaction with reduced sites. It is felt that this model is applicable to other copper-oxide-based catalysts, provided that special care is taken to maintain the system in an oxidized state. In a subsequent article it will be shown that the model forms a good basis to describe the reduction of NO by CO.

Acknowledgment

The authors would like to thank the Dutch Ministry of Environmental Affairs and P.S.A. France for their financial support.

Notation

$[A]$ = partial pressure of A, kPa
d_p = particle diameter, mm
E_{ai} = activation energy of process i, kJ·mol^{-1}
F_{Ao} = molar flow rate of A in feed, mol^{-1}
ΔH_i = enthalpy change over process i, kJ·mol^{-1}
k_i = rate constant of process i, kPa^{-1}·s^{-1}
k_{oi} = preexponential factor of rate constant k_i, kPa^{-1}·s^{-1}
K_i = equilibrium constant of process i, kPa^{-1}
K_{oi} = preexponential factor of K_i, kPa^{-1}
N_t = total active site density, mol/g
$O.F.$ = objective function for minimization
r_i = reaction rate of process i, mol·g^{-1}·s^{-1}
R = gas constant (8.314 J/mol·K), J·mol^{-1}·K^{-1}
s = number of neighbors of an active site
S_a = surface area of catalyst, m^2/g
T = temperature, K
T_{avg} = average temperature (460 K) over experimental conditions, K
$VHSV$ = volume hourly space velocity, h^{-1}
V_p = pore volume of catalyst, mL/g
W = catalyst weight, g
X_A = observed conversion of A
$\hat{X}_A$ = calculated conversion of A

Greek letter

θ_A = fractional surface coverage by A

Subscripts

A = component name
i = process number

Literature Cited

Balkenende, A. R., "Copper Catalyzed Reduction of Nitric Oxide," PhD Thesis, Utrecht, The Netherlands (1990).

Bijsterbosch, J. W., J. C. Muijsers, A. D. van Langeveld, F. Kapteijn, and J. A. Moulijn, "*In-Situ* FTIR Spectroscopy of Cu-Cr Catalysts in CO Oxidation," *Fundamental Aspects of Heterogenous Catalysis Studied by Particle Beams*, H. H. Brongersma and R. A. van Santen, eds., Plenum, New York in press (1992).

Boudart, M., D. E. Mears, and M. A. Vannice, *Ind. Chim. Belge*, Special Issue, **32**, 281 (1967).

Busca, J., "FT-IR Study of the Surface of Copper Oxide," *J. Mol. Catal.*, **43**, 225 (1987).

Carberry, J. J., *Catalysis, Science & Technology*, Vol. 8, p. 131, J. R. Anderson and M. Boudart, eds., Springer Verlag, New York (1987).

Choi, K. I., and M. A. Vannice, "CO Oxidation over Pd and Cu Catalysts," *J. Catal.*, **127**, 465 (1991).

Chu, C. F., and K. M. Ng, "Flow in Packed Tubes with a Small Tube to Particle Diameter Ratio," *AIChE J.*, **35**, 148 (1989).

Conner, W. C., and C. O., Bennett, "Carbon Monoxide Oxidation on Nickel Oxide," *J. Catal.*, **41**, 30 (1976).

Davydov, A. A., *Infrared Spectroscopy of Adsorbed Species on the Surface of Transition Metal Oxides*, C. H. Rochester, ed., Wiley, Chichester (1990).

Deen, R., P. I. Th. Scheltus, and G. de Vries, "Electron Paramagnetic Resonance of Supported Copper Oxide Catalyst in the Reduction of Nitric Oxide," *J. Catal.*, **41**, 218 (1976).

Dell, R. M., F. S. Stone, and P. F. Tiley, "The Decomposition of Nitrous Oxide by Cuprous Oxide and Other Oxide Catalysts," *Trans. Farad. Soc.*, **49**, 201 (1953).

Duprez, D., Z. Ferhat-Hamida, and M. M. Bettahar, "Surface Mobility and Reactivity of Oxygen Species on a Copper-Zinc Catalyst in Methanol Synthesis," *J. Catal.*, **124**, 1 (1990).

Dwyer, F. G., "Catalysis for Control of Automotive Emissions," *Catal. Rev.*, **6**, 261 (1972).

Eckert, E., V. Hlavacek, and M. Marek, "Catalytic Oxidation of CO on CuO/Al_2O_3: 1. Reaction Rate Model Discrimination," *Chem. Eng. Commun.*, **1**, 89 (1973).

Evans, J. W., M. S. Mainwright, A. J. Bridgwater, and D. J. Young, "On the Determination of Copper Surface Area by Reaction with Nitrous Oxide," *Appl. Catal.*, **7**, 75 (1983).

Froment, G. F., and L. H., Hosten, *Catalysis, Science and Technology*, Vol. 2, p. 40, J. R. Anderson and M. Boudart, eds., Springer Verlag, New York (1981).

Froment, G. F., and K. B. Bischoff, *Chemical Reactor Analysis and Design*, 2nd ed., Wiley, New York (1990).

Giamello, E., B. Fubini, P. Lauro, and A. Bossi, "A Microcalorimetric Method for the Evaluation of Copper Surfaces Area in Cu-ZnO Catalysts," *J. Catal.*, **87**, 443 (1984).

Gierman, H., "Design of Laboratory Hydrotreating Reactors Scaling Down Trickle-flow Reactors," *Appl. Catal.*, **43**, 277 (1988).

Gruzalski, G. R., D. M. Zehner, and J. F. Wendelken, "An XPS Study of Oxygen Adsorption on Cu(110)," *Surf. Sci.*, **159**, 353 (1983).

Habraken, F. H. P. M., and G. A. Bootsma, "The Kinetics of the Interaction of O_2 and N_2O with a Cu (110) Surface and of the Reaction of CO with Adsorbed Oxygen Studied by means of Ellipsometry, AES and LEED," *Surf. Sci.*, **87**, 333 (1979).

Habraken, F. H. P. M., C. M. A. M. Mesters, and G. A. Bootsma, "The Adsorption and Incorporation of Oxygen on Cu(100) and Its Reaction with Carbon Monoxide: Comparison with Cu (111) and Cu (110)," *Surf. Sci.*, **97**, 264 (1980).

Halasz, I., A. Brenner, M. Shelef, and K. Y. S. Ng, "Oxidation of Carbon Monoxide over Barium Cuprate Catalysts," *Catal. Lett.*, **6**, 349 (1990).

Happel, J., S. Kiang, J. L Spencer, S. Oki, and M. A. Hnatow, "Transient Rate Studies in Heterogeneous Catalysis: Oxidation of Carbon Monoxide," *J. Catal.*, **50**, 429 (1977).

Hertl, W., and R. J. Farrauto, "Mechanism of Carbon Monoxide and Hydrocarbon Oxidation on Copper Chromite," *J. Catal.*, **29**, 352 (1973).

Hupkens, Th.M., J. M. Fluit, and A. Niehaus, "LEIS Study of the Adsorption of Oxygen on a Cu(110) Surface, Stage II: Coverage above half a monolayer," *Surf. Sci.*, **165**, 327 (1986).

Jackson, S. D., "Isotopic Exchange of Carbon Dioxide and its Interaction with Carbon Monoxide over Copper Catalysts," *J. Catal.*, **115**, 247 (1989).

Kinnaird, S., G. Webb, and G. C. Chinchen, "Radiotracer Studies of Chemisorption on Copper-based Catalysts," *J. Chem. Soc. Farad. Trans.*, **84** 2135 (1988).

Kobayashi, M, T. Kanno, and Y. Konishi, "Dynamic Kinetics of CO Oxidation over Magnesium Oxide," *J. Chem. Soc. Farad. Trans.*, **83**, 721 (1987).

Kobayashi, M., T. Kanno, and T. Kimura, "Carbon Monoxide Oxidation Kinetics on Zinc Oxide," *J. Chem. Soc. Farad. Trans.*, **84**, 2099 (1988).

Krupay, B. W., and R. A. Ross, "The Catalytic Reaction between Carbon Monoxide and Nitrous Oxide over Chromium(III)oxide," *Can. J. Chem.*, **57**, 718 (1978).

Laine, J., J. Brito, and F. Severino, "Surface Copper Enrichment by Reduction of Copper Chromite Catalyst Employed for Carbon Monoxide Oxidation," *Catal. Lett.*, **5**, 45 (1990).

Laine, J., and F. Serverino, "Changes in Alumina-Supported Copper and Copper-Chromite Catalysts by the Introduction of Water during Carbon Monoxide Oxidation," *Appl. Catal.*, **65**, 253 (1990).

Liao, P. C., J. J. Carberry, T. H. Fleisch, and E. E. Wolf, "CO Oxidation Activity and XPS Studies of $Pt\text{-}Cu/\gamma\text{-}Al_2O_3$ Bimetallic Catalysts," *J. Catal.*, **74**, 307 (1982).

Lory, E. C., "The Catalytic Activity of Chromites for the Oxidation of Carbon Monoxide," *J. Phys. Chem.*, **37**, 685 (1933).

Luys, M. J., P. H. van Oeffelt, W. G. J. Brouwer, A. P. Pijpers, and J. J. F. Scholten, "Surface and Subsurface Oxidation of Copper and Supported Copper Catalysts by Nitrous Oxide," *Appl. Catal.*, **46**, 161 (1989).

Madhusudhan Rao, V., and V. Shankar, "Characterization of Supported Copper Catalysts for Methanol Dehydrogenation Prepared from Silica Hydrogel," *Appl. Catal.*, **45**, 335 (1988).

McCabe, R. W., and P. J. Mitchell, "Exhaust-Catalyst Development for Methanol-Fueled Vehicles," *Appl. Catal.*, **44**, 73 (1988).

Miro, E. E., D. R. Ardiles, E. A. Lombardo, and J. O. Pentunchi, "Continuous-Stirred Tank Reactor (CSTR) Transient Studies in Heterogeneous Catalysis," *J. Catal.* **97**, 43 (1984).

Miro, E. E., E. A. Lombardo, and J. O Pentunchi, "Kinetics and

Mechanism of CO Oxidation over Cu Mordenite," *J. Catal.*, **104**, 176 (1987).
Pentunchi, J. O., and W. K. Hall, "Studies of a CuY Zeolite as Redox Catalyst," *J. Catal.*, **80**, 403 (1983).
Press, W. H., B. P. Flannery, S. A. Teukolsky, and W. T. Vetterling, *Numerical Recipes*, Cambridge University Press, Cambridge (1989).
Schiavello, M., F. Pepe, and S. deRossi, "The Catalytic Activity of Copper Ions in Copper Oxides and in Their Solid Solutions with ZnO and MgO for the Decomposition of N_2O," *Z. Physic. Chem. N. F.*, **92**, 109 (1974).
Schlatter, J. C., R. L. Kimisch, and K. C. Taylor, "Exhaust Catalysts: Appropriate Conditions for Comparing Platinum and Base Metal," *Sci.*, **179**, 798 (1973).
Severino, F., and J. Laine, "Effect of Composition and Pretreatments on the Activity of Copper-Chromium-Based Catalysts for the Oxidation of Carbon Monoxide," *Ind. Eng. Chem. Prod. Res. Dev.*, **22**, 396 (1983).
Severino, F., J. Brito, O. Carias, and J. Laine, "Comparative Study of Alumina-Supported CuO and $CuCr_2O_4$ as Catalysts for the CO Oxidation," *J. Catal.*, **102**, 172 (1986).
Shelef, M., K. Otto, and H. Gandhi, "The Oxidation of CO by O_2 and by NO on Supported Chromium Oxide and Other Metal Oxide Catalysts," *J. Catal.*, **12**, 361 (1968).
Spitzer, A., and H. Lüth, "Adsorption and Dissociation of N_2O on Copper Single-crystal Surfaces," *Phys. Rev. B*, **30**, 3098 (1984).
Stegenga, S., N. J. J. Dekker, J. W. Bijsterbosch, F. Kapteijn, J. A. Moulijn, C. Belot, and R. Roche, "Catalytic Automotive Pollution Control without Noble-metals," *Studies in Surfaces Science and Catalysis*, A. Crucq and A. Frennet, eds., Elsevier, Amsterdam (Sept. 1991).
Stegenga, S., "Automotive Exhaust Catalysis without Noble Metals; a Search for an Alternative," PhD Thesis, Univ. of Amsterdam, The Netherlands (Sept., 1991).
Thomas, N. T., L. S. Caretto, and K. Nobe, "Catalytic Combustion of Carbon Monoxide on Copper Oxide," *Ind. Eng. Chem. Prod. Res. Dev.*, **8**, 282 (1969).
Tonner, S. S., M. S. Wainwright, O. L. Trimm, and N. W. Cant, "Characterization of Copper Chromite Catalysts for Methanol Dehydrogenation," *Appl. Catal.*, **11**, 93 (1984).
Winter, E. R. S., "The Decomposition of Nitrous Oxide in Metallic Oxides: II," *J. Catal.*, **19**, 32 (1970).
Yu Yao, Y. F., "The Oxidation of CO and C_2H_4 Over Metal Oxides," *J. Catal.*, **39**, 104 (1975).
Yu Yao, Y. F., and J. T. Kummer, "A Study of High Temperature Treated Supported Metal Oxide Catalysts," *J. Catal.*, **46**, 388 (1977).

Appendix A: Eq. 1 Derived from the Calculation of CO Conversion

In this derivation $a = CO_{2\,in}/CO_{in}$ and $b = CO_{2\,out}/CO_{out}$. The C-mass balance over the catalyst bed is given by:

$$CO_{in} + CO_{2\,in} = CO_{in}(1+a) = CO_{out} + CO_{2\,out} = CO_{out}(1+b) \quad \text{(A1)}$$

In combination with $CO_{out} = CO_{in}\,(1 - X_{CO})$, Eq. A2 is obtained.

$$CO_{in}(1+a) = CO_{in}(1-X_{CO})(1+b) \quad \text{(A2)}$$

Division of Eq. A2 by CO_{in} and substitution of a and b results in Eq. 1.

Appendix B: Rate Equations Derived for the Oxidation of CO by O_2 and N_2O

In the Appendix, the derivation of the rate equations of r_{CO} and r_{N_2O} of the selected model is given. This model consists of the following elementary processes:

k_1	$O_2 + 2\,\blacksquare \rightarrow 2\,O\text{-}\blacksquare$
k_2	$N_2O + \blacksquare \rightarrow O\text{-}\blacksquare + N_2$
k_3	$CO + O\text{-}\blacksquare \rightarrow CO_2\text{-}\blacksquare$
k_6, k_{-6}	$CO_2 + \blacksquare \rightleftharpoons CO_2\text{-}\blacksquare$
K_7	$CO_2 + O\text{-}\blacksquare \rightleftharpoons CO_3\text{-}\blacksquare$

Based on the assumption of a homogeneous surface, the rate of processes 1, 2, 3 and 6 equations can be expressed by Eqs. B1-B4.

$$r_1 = k_1 s\, N_t [O_2]\theta_{\blacksquare}^2 \quad \text{(B1)}$$

$$r_2 = k_2 N_t [N_2O]\theta_{\blacksquare} \quad \text{(B2)}$$

$$r_3 = k_3 N_t [CO]\theta_{O\text{-}\blacksquare} \quad \text{(B3)}$$

$$r_6 = k_6 N_t [CO_2]\theta_{\blacksquare} - k_{-6} N_t \theta_{CO_2\text{-}\blacksquare} \quad \text{(B4)}$$

The quasi-steady-state assumption for the surface intermediates $d\theta_i/dt = 0$ gives Eqs. B5-B7:

$$\theta_{O\text{-}\blacksquare} = \frac{2\,k_1 s\, N_t [O_2]\theta_{\blacksquare}^2 + k_2 N_t [N_2O]\theta_{\blacksquare}}{k_3 N_t [CO]} \quad \text{(B5)}$$

$$\theta_{CO_2\text{-}\blacksquare} = \frac{k_3}{k_{-6}}[CO]\theta_{O\text{-}\blacksquare} + K_6\theta_{\blacksquare}[CO_2] \quad \text{(B6)}$$

$$\theta_{CO_3\text{-}\blacksquare} = K_7[CO_2]\theta_{O\text{-}\blacksquare} \text{ (in equilibrium)} \quad \text{(B7)}$$

The total sum of these fractions must be 1 (Eq. B8):

$$\theta_{\blacksquare} + \theta_{O\text{-}\blacksquare} + \theta_{CO_2\text{-}\blacksquare} + \theta_{CO_3\text{-}\blacksquare} = 1 \quad \text{(B8)}$$

After substitution of Eqs. B5-B7 in Eq. B8 Eq. B9 is obtained:

$$a\,\theta_{\blacksquare}^2 + b\,\theta_{\blacksquare} + c = 0 \quad \text{(B9)}$$

where

$$a = \frac{2\,k_1 O_2 N_t}{k_3 CO}\left(1 + \frac{k_3}{k_{-6}}CO + K_7 CO_2\right) \quad \text{(B10)}$$

$$b = \frac{k_2 N_2O}{k_3 CO}\left(1 + \frac{k_3}{k_{-6}}CO + K_7 CO_2\right) + 1 + K_6 CO_2 \quad \text{(B11)}$$

$$c = -1 \quad \text{(B12)}$$

By using the positive root of Eq. B9 $\theta_{\blacksquare}$ can be calculated, after which $\theta_{O\text{-}\blacksquare}$ can be calculated by Eq. B5. The reaction rate of CO and N_2O is determined by Eqs. B13 and B14, respectively.

$$r_{CO} = k_3 N_t [CO]\theta_{O\text{-}\blacksquare} \quad \text{(B13)}$$

$$r_{N_2O} = k_2 N_t [N_2O]\theta_{\blacksquare} \quad \text{(B14)}$$

The derivation for the rate equations of r_{CO} and r_{N_2O} for the CO oxidation by O_2 or N_2O solely is identical under the omis-

sion of N_2O or O_2, respectively. Under the assumption that the reoxidation of the catalyst by O_2 is much faster than the reduction by CO (zeroth-order in O_2, $\theta_{\blacksquare}$ negligible compared to $\theta_{O\text{-}\blacksquare}$), the rate equation reduces to:

$$r_{CO(+O_2)} = \frac{k_3 N_t [CO]}{1 + \frac{k_3}{k_{-6}} [CO] + K_7 [CO_2]} \tag{B15}$$

The reaction rate equation of N_2O for the CO oxidation by solely N_2O is given by:

$$r_{N_2O(+CO)} = \frac{k_2 N_t [N_2O]}{1 + K_6 [CO_2] + \frac{k_2 [N_2O]}{k_3 [CO]} \left(1 + \frac{k_3}{k_{-6}} [CO] + K_7 [CO_2]\right)} \tag{B16}$$

Manuscript received July 2, 1991, and revision received Dec. 19, 1991.